



PHYSICS

SYNTHESIS AND CHARACTERIZATION OF NANO ZINC OXIDE BY SOL GEL SPIN COATING

K. Balachandra Kumar^{1*} and P. Raji²

¹Department of Physics, Kamaraj College of Engineering and Technology, Virudhunagar- 626 001, Tamilnadu, India

²Department of Physics, Mepco Schlenk Engineering College, Sivakasi – 625 005, Tamilnadu, India

Abstract

ZnO thin film has been deposited onto FTO glass substrate by the sol-gel spin coating method. Zinc acetate dehydrate, 2-methoxyethanol and monoethanolamine are used as a starting material, solvent and stabilizer, respectively. Dropping the coating solution into FTO substrate rotated at 3000 rpm for 20 sec using a spin coater. After the spin coating process the film is allowed to dry at 300°C for 10 min in a furnace to evaporate the solvent and to remove organic residuals. The XRD and SEM measurements confirmed that the thin films grown by sol-gel technique have good crystalline hexagonal wurtzite structure and homogenous surfaces. The optical absorbance of the deposited films is characterized by UV-VIS-NIR spectrometry. The optical band gap of deposited films is found to be 3.44 eV. The photoluminescence, FTIR and Raman spectra were studied and reported.

Keywords: Sol – gel Spin coating, FTO, ZnO, XRD, SEM, TEM, UV, PL, FTIR, Raman spectra

Introduction

Zinc oxide (ZnO) is a wide direct band-gap (3.37 eV) semiconductor with a broad range of applications including light-emitting devices [1], varistors [2], solar cells [3] and gas sensors [4]. Moreover, ZnO is a promising material for short wavelength optoelectronic devices, especially for ultraviolet (UV) Light-Emitting Diodes (LEDs) and Laser Diodes (LDs), due to its large exciton binding energy of 60 meV [5]. This exciton binding energy is much larger than the room temperature thermal energy (26 meV), suggesting that the electron-hole pairs are stable even at room temperature.

Therefore, an accurate knowledge of the structural and optical properties of ZnO is indispensable for the design and analysis of various optical and optoelectronic devices. The structural and optical properties of ZnO thin films depend on the preparation methods, substrate temperature, substrate material and subsequent annealing treatment [6–9]. Above all, the selection of substrate is very important for the growth of thin film because the matching in lattice parameters and crystal structure between the film and substrate strongly affects the crystal growth behavior of the film [10]. Fluorine Doped Tin Oxide (FTO) glass substrate has many excellent properties, such as electrical conductive and optical transparency, high Vis.-NIR light transmission, uniform transmission homogeneity and reflection in the infrared range. Since there is a small lattice mismatch (3%) between the neighboring oxygen–oxygen (O–O) distance on the closet-packed FTO (111) and ZnO (001) planes [11], and O dangling bonds on the FTO layer surface, it

benefits the initial nucleation and the subsequent growth of high quality ZnO films on FTO substrate.

ZnO thin films are currently fabricated by chemical vapor deposition [12], pulsed laser deposition [13], Molecular beam epitaxy [14], chemical spray hydrolysis [15], or other high-temperature and in some cases capital- and equipment intensive methods. Amongst the different available techniques, the sol-gel technique has the advantage of coating on large areas with easy control of the doping level, solution concentration and homogeneity, without using expensive and complicated equipment compared with other methods.

The results on the thin films of ZnO grown by sol-gel method have been presented. This technique of film preparation is a low-cost process and is attractive as the film properties can be tailored conveniently for a given application. This process, thus, becomes a preferred option for exploratory studies where a large number of candidate materials require screening for their compositions and properties prior to their applications in devices.

In the present work, we report the structural, optical and thermal properties of ZnO thin films prepared by sol-gel method using spin coating technique. Recently, few studies had reported on the growth of the ZnO thin film on FTO glass substrate.

Experimental

High purity stannous chloride ($\text{SnCl}_4 \cdot 5 \text{H}_2\text{O}$) is used as the source for tin. The fluorine doping was achieved using ammonium fluoride (NH_4F). Microscopic glass slide (75 x25 x1.4 mm³) is used as

* Corresponding Author, Email: dkbaldr@rediffmail.com

substrate. The substrate is cleaned using distilled water and various organic solvents.

The sol is prepared by dissolving 13 grams (0.37mole) of tin chloride ($\text{SnCl}_4 \cdot 5\text{H}_2\text{O}$) in 100 ml of ethyl alcohol. Ammonium fluoride (NH_4F) is then added into the solution. The amount of NH_4F added is 0.02275 moles, which corresponds to the $[\text{F}] / [\text{Sn}]$ ratio of 7.5at % [16]. To increase the solubility of the solute and to induce the simultaneous condensation and gelation, 5ml of 0.1N concentrated HCL is then added into the solution as a catalyst. The mixed solutions are well stirred and refluxed for one hour at 60°C . The solutions are cooled in the ambient and then aged in open beakers at room temperature, for gelation. 3 ml of the as prepared coated on the glass substrate by spin coater, which is spinned at 3000 rpm for 10 sec. The number of coatings is optimized to 10, in order to get films of good electrical and optical properties. Then the coated film is heat treated in a furnace at temperatures 325°C for about 30 minutes.

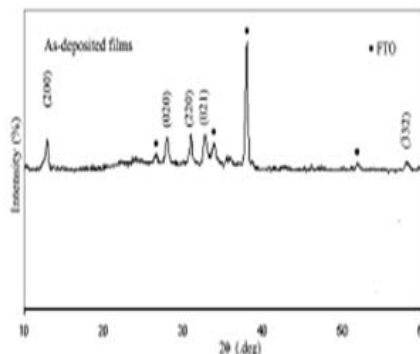
Zinc acetate dehydrate is first dissolved in mixture of 2-methoxy ethanol and monoethanolamine at room temperature. The sol is prepared by dissolving 8.23 grams (0.75 moles) of zinc acetate and the molar ratio of monoethanolamine to zinc acetate is kept at 1:1. The resultant solution is stirred for 1hr at 60°C to yield a homogeneous, clear and transparent solution using a magnetic stirred. The seed layers are spin coated a day after the solution is prepared. Precursor solution is dropped onto coming glass substrate, which are then spinned at 3000 rpm for 20 sec. The procedure was repeated for 5 times. After processing, the substrate is baked at 350°C for 10min to evaporate the solvent and remove the organic component in the film.

Characterization

XRD

Fig.1 shows the diffraction pattern of deposited film on FTO. It can be seen that the deposited film has nearly similar peak intensity for peak corresponding to (200), (020), (220) and (021) plane. The planes of (200), (020) and (220) indicate atoms are arranged in c -axis while (021) plane indicates atomic arrangement in a -axis. The film exhibits good crystallinity and all the peaks are indexed for a hexagonal ZnO lattice. These observed 'd' values are in good agreement with standard 'd' values. All the strong peaks are assigned to the pure hexagonal phase of wurtzite ZnO with calculated cell constants of $a = 3.245 \text{ \AA}$ and $c = 5.214 \text{ \AA}$ which are in good agreement with the reported standard values (JCPDS no.36 – 1451). The average crystallite size has been calculated with Scherrer relation was 43nm.

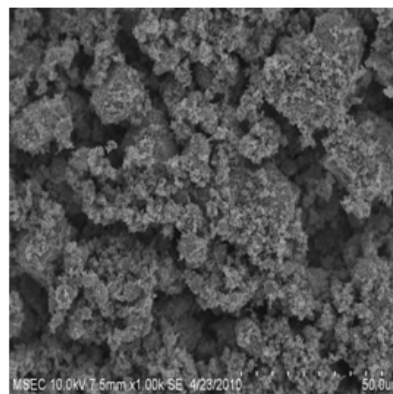
Fig.1. XRD of ZnO on FTO substrate



Surface Morphology

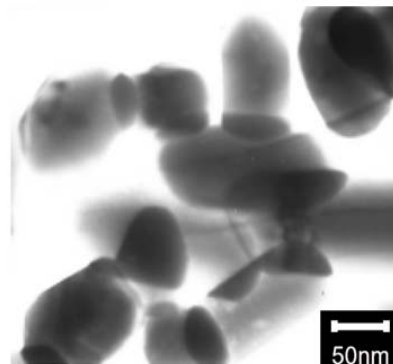
Fig.2.a shows the SEM image of as grown ZnO film deposited on FTO substrate. The film deposited in the optimized condition is smooth, dark gray in colour and uniformly covering the substrate with good adherence. The overall surface structure shows grains of spherical shape uniformly covering the substrate without any cracks and pores.

Fig.2.a SEM of ZnO on FTO substrate



A TEM image of the nanosize particle is given in Fig.2.b. It was observed clearly the particle size was about 50nm.

Fig.2.b. TEM image of ZnO film



UV-Visible Spectrum

The absorbance spectrum of ZnO thin films is shown in Fig.3 (a). From Fig.3 (a) it is seen that strong absorption occurs in UV wavelength at 360 nm. The weak absorption area covers almost the whole of the visible field ranging between 400 and 800 nm. The transmittance spectrum of the ZnO thin film shown in Fig. 3(b) reveals that the transmittance of the film is above 80 % in this visible region. The optical band gap of ZnO thin film is evaluated from the absorbance spectra of ZnO thin film on FTO coated glass. The substrate absorbance is corrected by introducing an uncoated FTO glass substrate of the same size for comparative study.

Fig.3.a. UV Vis Absorption spectrum of ZnO film

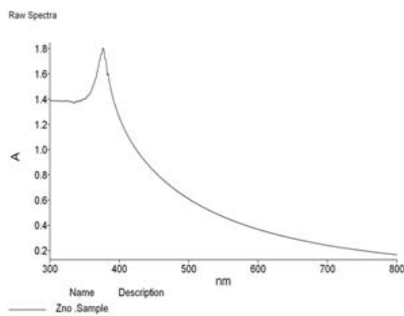
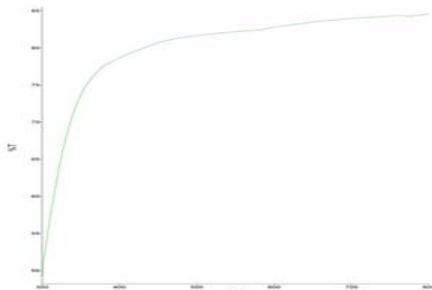


Fig.3.b. Transmission spectrum of ZnO film



The absorption coefficient of this film in this region is calculated using the following expression,

$$\alpha = 2.303 A / t$$

where, A is the absorbance and t is thickness.

The absorption coefficient α and the extinction coefficient k are related by the formula [17]

$$k = \alpha \lambda / 4\pi$$

The Optical energy gap E_g and absorption coefficient α are related by the equation

$$\alpha = (k/hv)(hv-E_g)^\beta$$

where, k is constant, h is Planck's constant, hv is the incident photon energy and β is a number which characterizes the nature of electronic transition between valance band and conduction band [18]. For direct allowed transitions $\beta = 1/2$ and it is known that

ZnO is a direct bandgap semiconductor. Therefore the formula used is

$$\alpha = (k/hv)(hv-E_g)^{1/2}$$

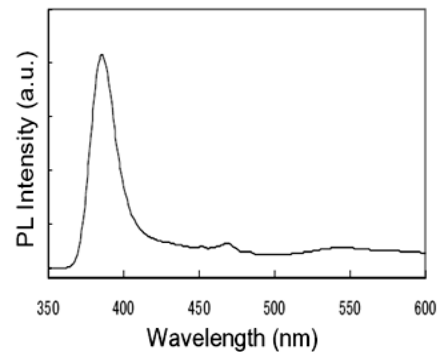
$$(ahv)^2 = C(hv-E_g)^{1/2}$$

where C is a constant. From the variation of $(ahv)^2$ vs. hv, energy gap E_g of the sample is estimated to be 3.44 eV.

PL spectrum

The room-temperature PL spectra of ZnO on FTO substrate was obtained with an excitation wavelength of 325 nm and is shown in Fig.4. In order to eliminate the interference from the substrate, those samples with maximal coverage are selectively used. A strong and sharp ultraviolet (UV) emission band dominates all the PL spectra. The UV emission also called the near band edge emission (NBE) at 3.24 eV may originate from free excitonic emission in the ZnO materials as ZnO has a high exciton-binding energy of 60 meV at room temperature. Visible light emission peak at around 2.65 eV is due to native defects such as interstitial zinc atoms, oxygen vacancies, ionized impurities, and lattice defects.

Fig.4. PL spectrum of ZnO film



Raman Spectrum

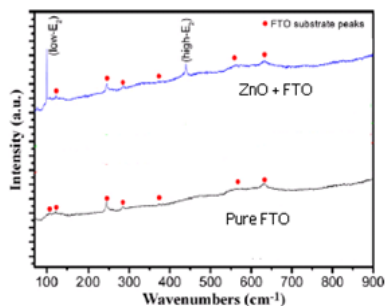
Raman measurements provide information about the material quality, the phase and purity, in order to understand transport properties and phonon interaction with the free carriers, which determine the device performances [19]. Considering the ZnO which belongs to the Wurtzite space group C_{6v}^4 , phonon modes E_2 (low and high frequency), A_1 [(TO)-transverse optical and (LO)-longitudinal optical] and E_1 (TO and LO) are expected all being Raman and infrared active. The optical phonons at the Γ point of the Brillouin zone belong to the representation [20]

$$\Gamma_{opt} = 1A_1 + 2B_1 + 1E_1 + 2E_2$$

The Raman spectrum from the FTO substrate itself is presented as a reference (Fig.5). It can be observed that the broad peaks at 106 cm^{-1} , 122 cm^{-1} , 244 cm^{-1} , 284 cm^{-1} , 373 cm^{-1} , 472 cm^{-1} , 494 cm^{-1} , 561 cm^{-1} , and 633 cm^{-1} arise from the FTO substrate and

can be found in all spectra of our sample. The noted E_2 (high) peak is one of the characteristic peaks of Wurtzite ZnO attributed to the high frequency E_2 mode [21] assigned to multiple-phonon processes. Dominant peaks at 100 cm^{-1} and 438 cm^{-1} , which are commonly detected in the wurtzite structure ZnO, are attributed to the low- and high- E_2 mode, respectively of non-polar optical phonons. The Raman spectrum of as-grown ZnO film exhibits a resolved peak centered at 438 cm^{-1} corresponding to high frequency E_2 (high) mode in ZnO.

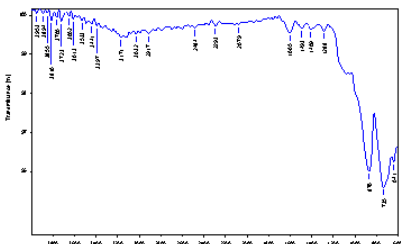
Fig.5. Raman spectrum of ZnO film



FTIR

Fig. 6 shows the FT-IR spectra of ZnO thin film, absorption bands near 3411 cm^{-1} represent O-H mode, those at 2911 cm^{-1} are C-H mode, and $1409\text{-}1605\text{ cm}^{-1}$ are the C=O stretching mode. As the temperature increases, the organic band at $1409\text{-}1605\text{ cm}^{-1}$ is removed, but the bands arising from the absorption of atmospheric CO_2 on the metallic cations at 2303 cm^{-1} and bonding between Zn-O (611 cm^{-1} , 735 cm^{-1}) are clearly represented.

Fig.6. FTIR of ZnO film

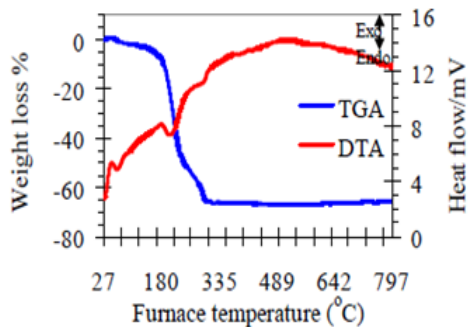


TG-DTA

The thermal behaviour of dried ZnO gel has been investigated by differential thermal analysis (DTA) and thermogravimetric analysis (TGA). The TG-DTA result is shown in Fig.7. Two weight losses are observed at about $50\text{-}100^\circ\text{C}$ and $175\text{-}300^\circ\text{C}$ in the TG curve. The first weight loss is due to the evaporation of water and 2-methoxyethanol. The second weight loss is caused by the decomposition of residual organics and MEA. Three endothermic peaks are found at 63°C , 202°C

and 291°C , respectively. These peaks are accompanied by the weight loss mentioned above. It is observed that there is no weight loss after the about 300°C . So, the preheating temperature is selected 300°C .

Fig.7. TG DTA for ZnO



Conclusions

To summarize, a high quality ZnO nanocrystalline film on FTO substrate has been prepared by sol gel method using spin coating technique. The structural and optical properties of ZnO film are studied. Maximum crystalline size is obtained as 43 nm and band gap energy is found 3.44 eV. XRD show that the film exhibited a single-crystalline wurtzite hexagonal structure. Room temperature PL spectra of the ZnO nanowires show a strong UV emission band located at 360 nm which was ascribed to the near band-edge emission. Finally properties of the ZnO thin films on FTO substrate can be very good, which makes this method promising for fabricating the optoelectronic nanodevices, such as LED and LD in Future.

References:

1. J. Gao, A.J. Heeger, J.Y. Lee, C.Y. Kim, *Synth. Met.* Vol.82 1996 pp.221-223.
2. N.T. Hung, N.D. Quang, S. Bernik, *J. Mater. Res.* Vol.16, 2001 pp.2817 -2823
3. N.F. Cooray, K. Kushiya, A. Fujimaki, D. Okumura, M. Sato, M. Ooshita, O. Yamase, *Jpn. J.Appl. Phys.* Vol.38, 1999 pp.6213 - 6218.
4. R. Paneva, D. Gotchev, *Sens. Actuat. A: Phys.* Vol.72 1999 pp.79 – 87 .
5. C.M. Lieber, *Solid State Commun.* Vol.107 1998 pp.607-616.
6. M. Zerdali, S. Hamzaoui, F.H. Teherani, D. Rogers, *Mater. Lett.* Vol.60 2006 pp.504 - 508 .
7. T.W. Kim, K.D. Kwack, H.K. Kim, Y.S. Yoon, J.H. Bahang, H.L. Park, , *Solid State Commun.* Vol. 127 2003 pp. 635 - 638.
8. I.S. Kim, S.H. Jeong, S.S. Kim, B.T. Lee, *Semicond. Sci. Technol.* Vol 19, 2004 pp.L29 .

9. K. Keem, H. Kim, G.T. Kim, J.S. Lee, B. Min, K. Cho, M.Y. Sung, S. Kim, *Appl. Phys. Lett.* Vol. 84 2004 pp. 4376-4380.
10. R. Ghosh, D. Basak, S. Fujihara, *J. Appl. Phys.* Vol.96, 2004 pp. 2689-2692 .
11. H. Yi, I. Yasui, Y. Shigesato, *Jpn. J. Appl. Phys.* Vol. 34 1995 pp. 1638-1642
12. H. Gomez, A. Maldonado, R. Asomoza, E.P. Zironi, J. Canetas-Ortega, J. Palacios-Gomez, *Thin Solid Films*, Vol.293 1992 pp. 117-123 T. Minami, H. Sato, H.Sohokara, S.Takata, T.Miyata, I. Fukuda, *Thin Solid Films*, Vol. 253 1994 pp. 14 -19 .
13. Ennaoui, A. Weber, R.Scheer, H.J. Lewerenz, *Sol. Energy Mater. Sol. Cells*, Vol. 54 1998 pp. 277-286
14. Y.L Liua, Y.C. Liua, Y.B. Liub, D.Z. Shena, Y.M. Lua, J.Y. Zhanga, X.W. Fana, *Solid State Communications*, Vol. 138 2006 pp. 521-525
15. A.N. Banerjee, S. Kundoo, P. Saha, K.K. Chattopadhyay, *Journal of Sol-Gel Science and Technology*, Vol.28_2003_pp. 105-110.
16. E.RShaaban, . *Journal of Applied Sciences*,Vol. 6 (2), 2006 pp.340 – 344
17. Li, Ming-Fu, *Modern Semiconductor Quantum Physics*, World Scientific, Singapore, (2001).
18. W. Limmer, W. Ritter, R. Sauer, B. Mensching, C. Liu, B. Rauschenbach, *Appl. Phys. Lett.* Vol. 72 1998 pp. 2589-2593.
19. C. Bundesmann, N. Ashkenov, M. Schubert, D. Spemann, T. Butz, E.M. Kaidashev, M. Lorenz, M. Grundmann, *Appl. Phys. Lett.* Vol. 83 2003 pp. 1974 – 1978 .
20. T.C. Damen, S.P.S. Porto, B. Tell, *Phys. Rev.* Vol.142,1996,pp.570-575.